ACADEMIA ROMÂNĂ
Revue Roumaine de Chimie
https://web.icf.ro/rrch/

Rev. Roum. Chim.,
2022, *67*(8–9), 493–501
DOI: 10.33224/rrch.2022.67.8-9.08

EVALUATION OF THE MICROORGANISMS GROWTH WITH STABILIZED DOXORUBICIN ON NANO GRAPHENE OXIDE SUBSTRATE

Sedigheh PARGALEH BOROUJENI,[a,b] Noureddin GOODARZIAN,[c] Neda HASANZADEH[B] and Mohammad Kazem MOHAMMADI[d,*]

[a]Department of Chemistry, Ahvaz Science and Research branch, Islamic Azad University, Ahvaz, Iran
[b]Department of Chemistry, Ahvaz Branch, Islamic Azad University, Ahvaz, Iran. Postal code: 61349-23653
[c]Department of Chemistry, Shiraz Branch, Islamic Azad University, Shiraz, Iran. Postal code: 71236-17628
[d]Advanced Surface Engineering and Nano Materials Research Center, Department of Chemistry, Ahvaz Branch, Islamic Azad University, Ahvaz, Iran

Received August 18, 2022

In order to measure the effect of graphene oxide-stabilized drug on the growth of microorganisms, first the graphene oxide used was prepared from graphite modified by Homers method. After preparation of graphene carrier, doxorubicin was loaded by ultrasound. Then, due to the high biocompatibility of drug carriers, their cytotoxicity and antibacterial properties were determined by the methods of minimum inhibitory concentration, minimum bactericidal concentration and plate penetration. The effect of prepared carriers containing metal nanoparticles on the growth of microorganisms such *Enterococcus*, *Corynebacterium* and *Escherichia coli* were studied as statistical means. The best minimum inhibitory concentration (MIC) values were obtained for Fe/Ag/M (rGO/Cis) nanoparticles, which had a lower minimum concentration compared to other nanoparticles or their combinations. Among these, the rGO/Cis sample had the best performance. Bacteria of *Corynebacterium* and *Enterococcus* showed the greatest reduction in viability against RGO / Cis up to 125 and 62.5 μg/mL, respectively. Carriers prepared in this study were generally not very toxic, as a high percentage of cells survived in the concentration range less than 100 μg/mL.

INTRODUCTION

Lung, bronchial, breast, and colorectal cancers are the most common causes of fatal cancers in women. According to statistics released in 2010, breast cancer alone accounts for 28% of all cancers in American women.[1,2] Cancer is one of the challenges in today's world and many people die every year due to this disease. The drugs used for treatment are usually nonspecific. Although chemotherapy plays an important role in the treatment of cancer, the use of anti-cancer agents has an adverse effect on normal tissue. Over the past two decades, new drug delivery system have been developed that have, to some extent, been able to alleviate the problems associated with the adverse effects of drugs. These systems include nanoparticles containing organic and inorganic compounds. Some of these systems, such as graphene substrate systems, are now making their way in to the pharmaceutical market, and many others are in the preclinical stages.[3–12] Doxorubicin is one of the drug treatments for cancer. Given the proven effects of this drug in the treatment of cancer, more research is needed to improve its function and convert it into a nanoparticle.[13–15]

The inhaled formulation of this drug prepared using polymer nanoparticles to prevent the side effects of the oral consumption and has clear advantages over the oral formulation. However, the

* Corresponding author: mkmohamadi@gmail.com

clinical use of doxorubicin is associated with acute and sub-acute side effects such as irreversible toxicity in the heart and other tissues[14, 15] and has made the use of this drug difficult.

During treatment, some cells become resistant, either as result of dosage increase during treatment or due to association with other drugs. To reduce the high toxicity of the drug, a variety of drug delivery system have been developed, including polymer, nanoparticle, and micro particle drug-soluble conjugates. Among these, nanoparticles have received more attention because they have an easier production method. Targeted nanoparticles can be used by placing specific ligands on the relevant surface to bind to specific cellular receptors and thus targeted drug delivery to specific cells. So far, nanoparticles have been shown to increase drug uptake by mechanisms such as endocytosis. Recently, nano-synthesized graphene oxide was investigated for drug delivery as a carrier for quercetin, a flavonoid with known nutritional and therapeutic properties. Graphene oxide is one of the most widely used nanostructured compounds in the field of production of intelligent drug carriers.[16, 17]

Surface modification of graphene oxide with different compounds in order to increase the loading efficiency and stabilization of the drug on it has been extensively studied.[18] The present study was performed due to the fact that so far there has been no report on the placement of this drug, which is effective on graphene oxide nanoparticles and improves its performance.

There are many studies related to the bactericidal effects and their inactivation by the doxorubicin, and it has been stated that its antibacterial mechanism is similar to the cytotoxicity effects on human cancer cells.[19] Because in the present study, a new formulation of this drug was prepared, we tried to study its antibacterial effects on *Staphylococcus aureus*, *Enterococcus Faecalis*, *Coryne bacterium* and *Escherichia Coli*.

EXPERIMENTAL

1. Material sand methods

Graphite was purchased from Merk. Concentrated sulfuric acid with 98% purity, sodium nitrate ($NaNO_3$), sodium sulfate (Na_2SO_4), potassium permanganate ($KMnO_4$) and 30% hydrogen peroxide (H_2O_2) were purchased from Merck, Germany. Doxorubicin hydrochloride was purchased from Merk.

Preparation of graphene oxidase drug carrier Modified Homers and of Man method was used to synthesize graphene oxide from natural graphite powder. Briefly, graphite (0.5 g), sodium nitrate $NaNO_3$ (0.5 g) and 23 mL of concentrated H_2SO_4 were mixed for 1 hour in an ice-water bath. Then 1.5 g $KMnO_4$was slowly added and the solution was stirred for one day at 35 ˚C. To the above mixture, 23 mL of distilled water was slowly added and stirred for 30 minutes with increasing temperature (but not exceeding 98 ˚C). Finally, 5 mL 30% H_2O_2 and 70 mL deionized water were added to the mixture. There action mixture was passed through as trainer and washed several times with 3% HCl and deionized water. This process was performed several times with centrifugation. Finally, the brown colored solid was dried in vacuum oven.

2. Graphene oxide reduction

Graphene oxide is usually not thermally stable, so it is partially reduced to increase the ratio of carbon atoms to oxygen. Chemical, thermal and multistage reduction of graphene oxide and rGO preparation methods. Thermal and chemical reduction is usually done in one step. In this study, chemical reduction with sodium borohydride was performed to prepare rGO from GO.

To loaded doxorubicin on to graphene oxide and reduced graphene oxide-based drug carriers, two milliliters of phosphate buffer and six milligrams of Nano composite were first sonicated for five minutes. Then 10 mL of doxorubicin with a certain concentration was added to it. Then, the suspension was stirred with a magnetic stirrer for 18 hours in a dark environment. The final product was washed by centrifugation and the supernatant was used for ultraviolet-light spectroscopy to determine the yield and loading efficiency of the drug. The drug loading percentage is calculated from the following equation.

$$L\% = \frac{w_1 - w_2}{w_{a,d}} \times 100 \qquad \text{eq. 1}$$

In this equation, W1 and W2 are the initial weight of the drug in the loading solution and the weight of the drug not loaded, respectively. The difference between the two is equal to the weight of the drug loaded. W is the absorbent weight for loading the drug.

3. Characterization of stabilized doxorubicin on nano graphene oxide substrate

3.1. Fourier-transform infrared spectroscopy (FTIR)

In order to confirm the syntheses and investigate the interactions between components in nano composite scaffolds, the FT-IR spectrum of the samples prepared by PIKE GladiATR attachment device (USA) in the range of 400–4000 cm^{-1}. For FT-IR analysis, tablets of samples with potassium bromide (KBr) were used.

3.2. X-ray powder diffraction (XRD)

In the present research, XRD analysis was used to confirm the conversion of the successful synthesis of graphene oxide and its reduction to rGO. The XRD patterns of the samples were recorded with the D8 ADVANCE device manufactured by Bruker (Germany) in the range of 2θ = 10–80˚, CuKα radiation equal to 8.04 keV and wavelength A˚ 1.54.

3.3. Field emission scanning electron microscopy (FESEM)

FESEM has been used to investigate the morphology of drug carriers based on graphene oxide and reduced graphene oxide.

4. Evaluation of anti-bacterial effects

4.1. Minimum inhibitory concentration (MIC)

Bacteria of *Staphylococcus aureus*, *Enterococcus faecalis*, *Corynebacterium* and *Escherichia coli* were used for this purpose. Then the effect of Graphene oxid/Doxorubicine compounds on the growth rate of these microorganisms in the micro dilution method and according to the instructions of the Clinical and Laboratory Standards Institute at concentrations of 500, 200, 100, 50, 10.1(g/mL) were tested in Muller Hinton or BHI medium.

For this purpose, each of the microorganisms was first cultured overnight in Muller-Hinton or BHI medium. And then transfer 10 µL of the bacterial suspension to the culture medium to a turbidity equivalent to 0.5 McFarland standard (OD_{600} = 0.11). The resulting bacterial suspension was diluted 20 times, and 10 µL of this suspension was added to 96-well plate wells containing 90 µL of Muller-Hinton or BHI medium with the desired concentrations of compounds. Wells containing Muller-Hinton or BHI medium without nanoparticles were considered as negative control wells and wells containing Muller-Hinton or BHI medium as positive control. The antibiotic ampicillin was used as the standard inhibitory drug. For each compound at each concentration, a well to which no bacterial suspension was added was considered a blank well. The plates were incubated at 37°C for 24 hours. In order to reduce evaporation in the incubator or, a tray containing sterile distilled water was placed in the incubator the day before. After incubation, the growth rate of bacteria was measured by turbidity using a micro plate reader (Bio Tek, Power Wave XS2) at 600 nm. The results were obtained as a percentage of bacterial viability using equation 1.

$$V = \frac{A_t - A_b}{A_c - A_b} * 100\% \qquad \text{eq. 2}$$

In this formula, V is the percentage of viable cells, A_t is the amount of adsorption in the test Wessel, A_b is the amount of adsorption in the control Wessel and A_c is the amount of adsorption in the control well.

4.2. Minimum bactericidal concentration (MBC)

MBC is considered as the lowest concentration that can kill 98% of bacteria. For MBC determination 10 µL of MIC concentration was poured on medium and incubated for 24 hours at 37˚C.

4.3. MCF7 cell line

MCF-7 breast cancer cell line was cultured according to the protocol provided by the cell bank of Pasteur Institute of Iran. Accordingly, the cells were cultivated in DMEM culture medium with 10% fetal bovine serum and penicillin/ streptomycin (100 µg/mL) in a CO_2 incubator (5% CO_2) at 35°C (1 x 10^5 cells/ml) in 96 plates for 24 h. After that, the cells were treated with formulations designed in current study.

5. Statistical analyses

In the present study, SPSS software Version 24 was used to analyze the data. To evaluate the results of biological experiments, the data in each group were presented as mean standard deviation and the significant difference between the means of the groups was analyzed by one-way analysis of variance (One-way ANOVA) and then Tukey test. In all tests, an average of 3 measurements was used for each group and a probability level of $P < 0.05$ was considered as significant difference.

RESULTS

1. Characterization of designed nanoparticles

1.1. FTIR

The FTIR spectrum of graphene oxide, reduced graphene oxide, GO-DOX and rGO-DOX can be seen in Fig. 1a. The peak in the region of 1716 cm^{-1} corresponds to the stretching vibration of the carbonyl group (C=O). The peaks related to the stretching vibration of aromatic ring hydrogens and C=C bonds in graphene oxide also appeared at 3117 cm^{-1} and 1577 cm^{-1}, respectively. These peaks well represent the structure of graphene oxide with high purity. The broad peak appearing in the region of 2500–13500 cm^{-1} is also related to the stretching vibration of OH hydrogen bonds on the surface of graphene oxide. In the reduced graphene oxide (rGO) spectrum, the peak at 2789 cm^{-1} corresponds to the stretching vibration of C-H bonds. The peak at 1731 cm^{-1} is related to the C=O bond in carbonyl groups such as carboxylic acid. The 1567 cm^{-1} peak is related to unreduced graphene oxide. The peak at 1200 cm^{-1} is also for the stretching vibration of the C-O bond.

FTIR spectrum of DOX, DOX-GO and DOX-rGO samples can be seen in Fig. 1b. In the spectrum of DOX-GO, the stretching vibration of the carbonyl group is observed at 1608 cm^{-1}, and this strong shift towards the lower wave number indicates the interaction of DOX with graphene oxide and the formation of DOX-GO. This shows that doxorubicin is well loaded on graphene oxide and the shift of the carbonyl group peak is caused by strong interactions such as hydrogen bonding between DOX and graphene oxide. The strong peak appearing at 1420 cm^{-1}, which is related to aromatic rings, is also shifted to lower wavenumbers under the influence of the interactions between DOX and GO.

1.2. XRD

The XRD patterns of GO and rGO are shown in Fig. 2a. XRD peak related to GO is in $2\theta = 11.6°$ with interlayer distance of 0.8 nm. However, this peak in rGO was seen in $2\theta = 25.4°$ with interlayer distance of 0.4 nm.

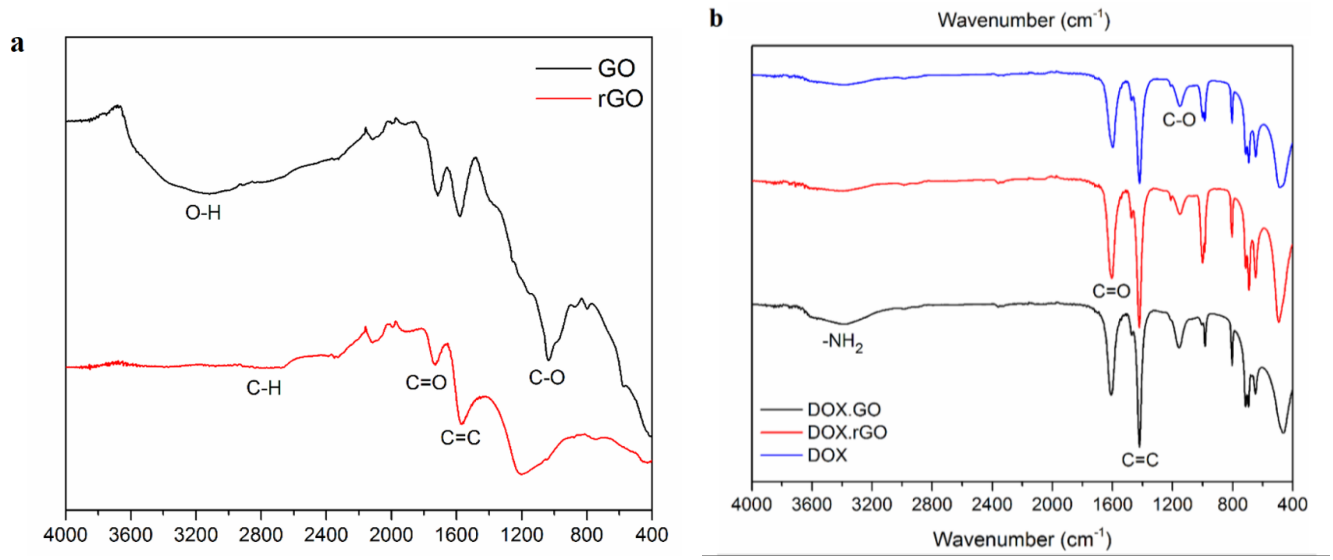

Fig. 1 – The FTIR spectra of graphene oxide (GO) and reduced graphene oxide (rGO) (a) and Doxorubicin (DOX), Doxorubicin graphene oxide (DOX-GO) and Doxorubicin reduced graphene oxide (DOX-rGO) (b).

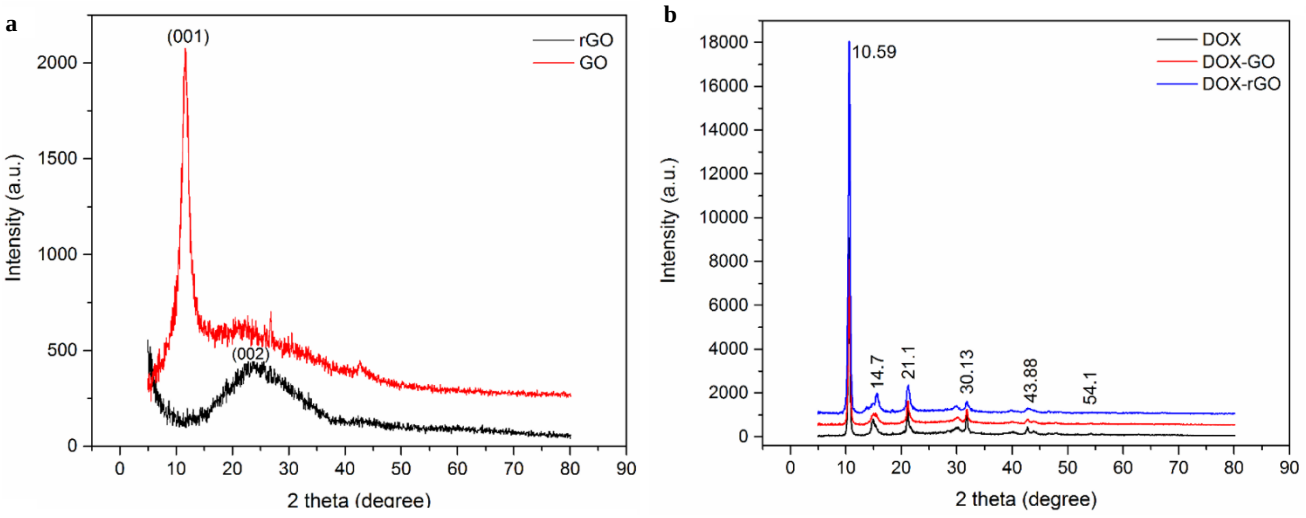

Fig. 2 – The XRD patterns of graphene oxide (GO) and reduced graphene oxide (rGO) (a) and Doxorubicin (DOX), Doxorubicin graphene oxide (DOX-GO) and Doxorubicin reduced graphene oxide (DOX-rGO) (b).

The XRD patterns of DOX, DOX-GO and DOX-rGO are shown in Fig. 1 b. XRD peak for DOX was in 2θ =10.59, 14.7, 21.1, 30.13, 43.88 and 54.1, which related to its crystalline structure. The XRD patterns of DOX-GO and DOX-rGO had the same patterns of both DOX and GO, indicating the successful loading of DOX in GO and rGO.

1.3. FESEM

The images of FESEM of GO, rGO, DOX-GO and DOX-rGO are shown in Fig. 3. As can be seen, the layering structures of both GO and rGO are evident. There was no change in the structure and morphology of formulations after loading the DOX in GO and rGO.

1.4. Effect of compounds on the growth of microorganisms

The results of antibacterial test a represented in Table 1. The best MIC values are obtained for Fe/Ag/M (rGO/Cis) nanoparticles, which have a lower minimum concentration compared to other nanoparticles or their combinations, in other words, they show higher efficiency. All samples concentrations (1000 μg/L) show strong antibacterial properties against all four types of bacteria studied. The results are the same for MBC. Fe/Ag/M (rGO/Cis) nanoparticles provide the lowest MBC valuesfor all four bacterial strains. All nanoparticles used in high concentrations (500 to 1000 μg/μL) show antibacterial properties.

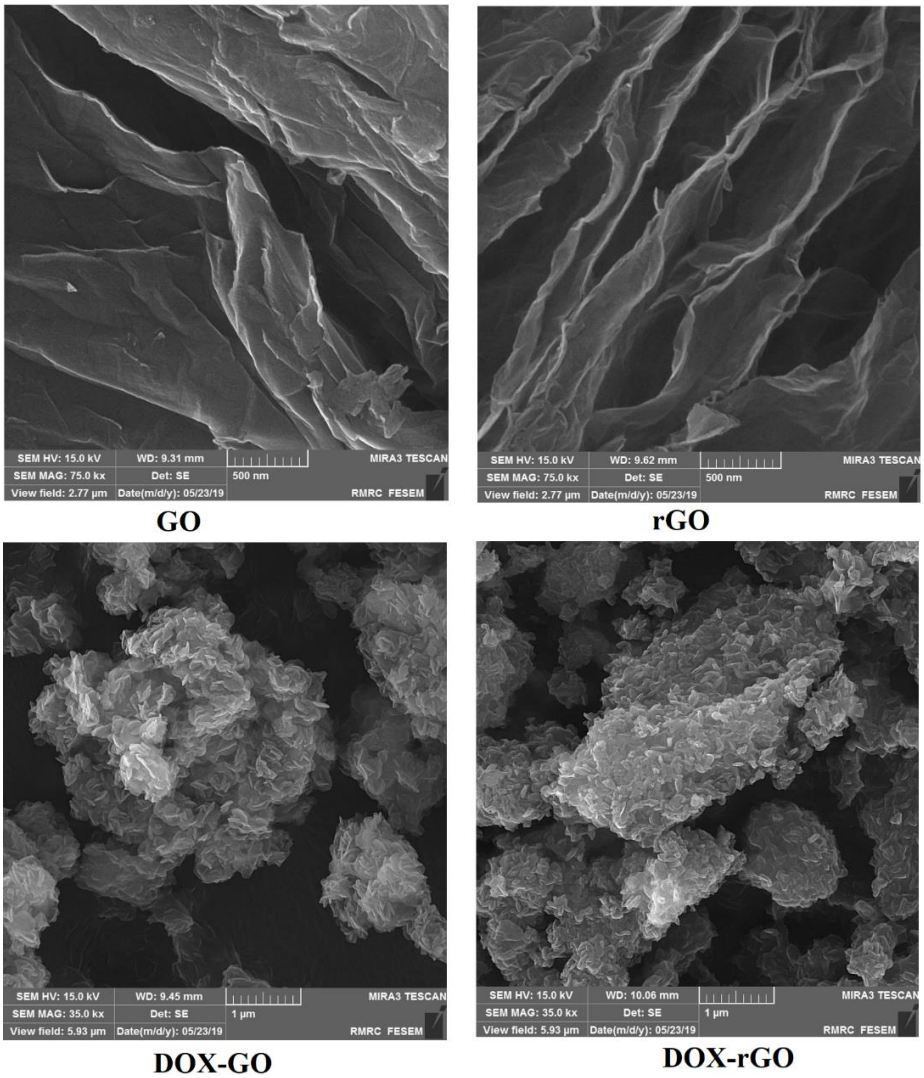

Fig. 3 – The Field emission scanning electron microscopy (FESEM) images from graphene oxide (GO), reduced graphene oxide (rGO), Doxorubicin (DOX), Doxorubicin graphene oxide (DOX-GO) and Doxorubicin reduced graphene oxide (DOX-rGO).

Table1
Antibacterial test results on synthesized nanoparticles

Fe/Ag/M (µg/mL) RGO/Cis		Fe/M (µg/mL) RGO/cabo		Fe/Ag (µg/mL) RGO/DOX		Ag/M (µg/mL) Go/cis		Fe (µg/mL) Go/carbo		Ag (µg/mL) Go/DOX		microorganisms
MBC	MIC	MBC	MIC	MBC	MIC	MBC	MIC	MBC	MIC	MBC	MIC	
125	62.5	1000	500	500	500	500	250	1000	1000	500	500	*Staphylococcus*
250	62.5	1000	500	500	500	250	125	1000	1000	250	250	*Enterococcus faecalis*
125	125	500	500	1000	1000	250	250	1000	1000	1000	500	*Corynebacterium*
250	125	500	250	250	250	125	62.5	1000	500	125	125	*Escherichia coli*

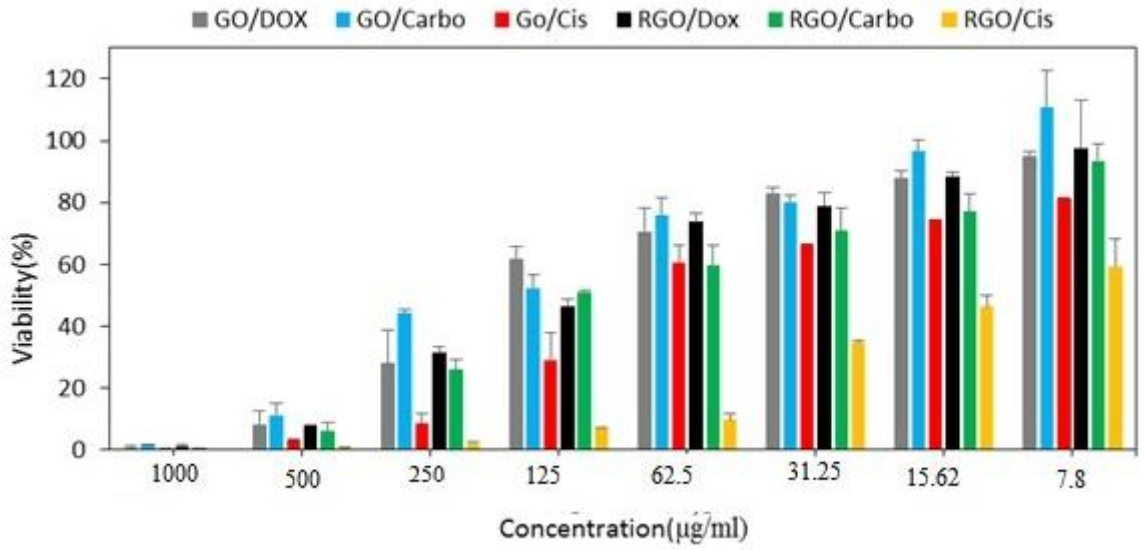

Fig. 4 – Antibacterial properties of GO/DOX, GO/carbo, GO/Cis, rGO/DOX, rGO/Carbo and RGO/Cis at different concentrations against *Staphylococcus aureus.*

2. The effect of synthesized nanoparticles on the growth of microorganisms

The effect of synthesized nanomaterials on microorganisms of *Staphylococcus aureus*, *Corynebacterium*, *Enterococcus faecalis* and *Escherichia coli* in concentrations of 7.8 to 1000 µg/mL was investigated by micro dilution method and the results were presented as mean life percentage standard deviation. Graphs related to the percentage of bacterial viability relative to the concentration of samples prepared in this study are presented here for better comparison and evaluation of antibacterial properties. Fig. 1 shows the corresponding diagram for *Staphylococcus bacteria*. At a concentration of 1000 µg/L, the percentage of living cells in almost all samples was close to zero. With decreasing concentration, the percentage of viable cells increased, which has the best performance of rGO/Cis sample.

The diagram showing the effect of rGO on *Enterococcus faecalis* is presented in Fig. 2. For this bacterium, all compounds in high concentrations (500 and 1000 µg/mL) significantly reduced the number of bacteria. In fact, by reducing the concentration from 1000 to 7.8 µg/mL, the antibacterial property also decreases to the extent that at the lowest concentration, bacterial growth can be observed. Among the compounds tested, it can be stated that the rGO/Cis compound showed a stronger antibacterial property against *Staphylococcus aureus* compared to other compounds. By comparing GO/DOX and GO/Cis compounds, it can be said that they are able to induce antibacterial properties in the compound. The same effect can be observed in Go/cis and RGO/Cis compounds and it was concluded that graphene oxide in combination with substances such as cisplatin can produce a strong antibacterial property so that up to a low concentration such as 62.5 µg/mL from this substance, death of over 90% of bacteria is noted.

The bacteria *Corynebacterium* and *Enterococcus* behave similarly to *Staphylococcus* (Figs. 4 and 5). The difference was that the rate of increase in life of these bacteria in response to low concentrations was significantly increased. These two bacteria also showed the greatest reduction in viability against RGO/Cis up to 125 and 62.5 µg/mL, respectively, and also with a similar argument can confirm the antibacterial behavior of this compound. By statistical analyses and comparison of the behavior of the three gram-positive bacteria, it can be stated that all behavioral compounds are almost similar to gram-positive bacteria and the results of three different antibacterial methods prove the theory that they can be a strong antibacterial.

Fig. 5 showed antibacterial properties of samples compared to bacterium *Corynebacterium*. In the case of gram-negative bacteria such as *Escherichia coli*, the general situation was somewhat different, so that only at a concentration of 1000 µg/mL all compounds were able to reduce the number of bacteria by 90%; by reducing the concentration from 1000 to 7.8 µg/mL not only the antibacterial effect was not reduced but we also saw a significant growth of bacteria. In this group

of bacteria, rGO/Cis showed the best antibacterial properties in comparison with other compounds because concentrations up to 125 μg/mL was able to kill more than 90% of bacteria. On the other hand, the presence of graphene oxide, especially at low concentrations, led to reduced bacterial growth. But in a compound like Go/ Car boat low concentrations we saw significant growth of bacteria. As can be seen from the figure, in all compounds, the antifungal property increases significantly with increasing concentration (Fig. 6).

3. Evaluation of cytotoxicity to MCF-7 cells

The toxicity of the samples to MCF-7 line cells for the three samples Cis,GO/Cis and rGo/ Cis is shown in Fig. 5. As the concentration of all three samples increased, the percentage of cell viability decreased, indicating that these samples had higher cytotoxicity thigh concentrations. At concentrations less than 200 μg/mL, cell viability was quite high. On the other hand, the cytotoxicity of rGO/Cis sample was higher compared to other samples. In fact, it can be said that these samples are generally not very toxic, especially in the concentration range of less than 100 μg/mL, 100% of the cells survived. The lowest rate of life with 21.76 was related to rGO/Cis sample in 500 μg/mL. The highest viability was related to Cis sample with a value of 109.45 at a concentration of 1 μg/mL.

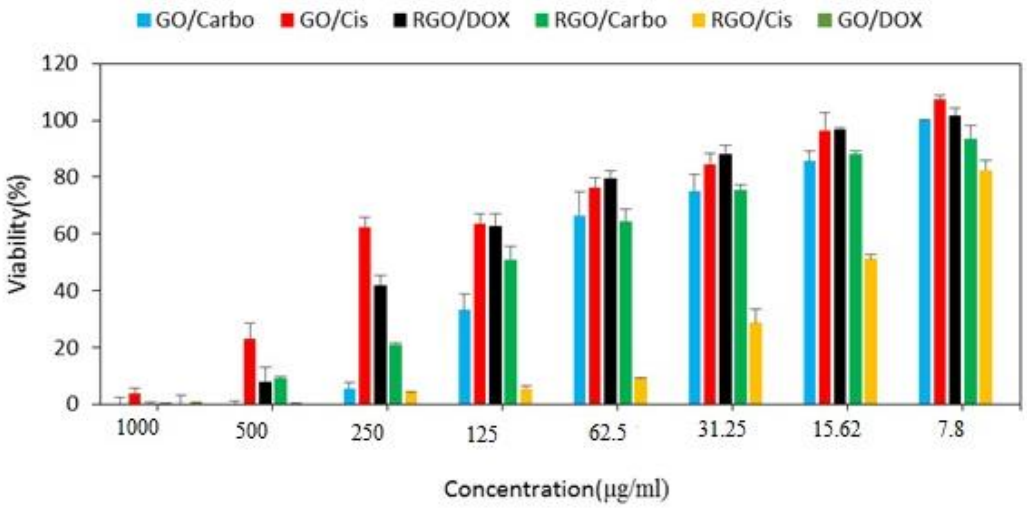

Fig. 5 – Antibacterial properties of of GO/DOX, GO/carbo, GO/Cis, rGO/DOX, rGO/Carbo and RGO/Cis at different concentrations against *Enterococcus faecalis*.

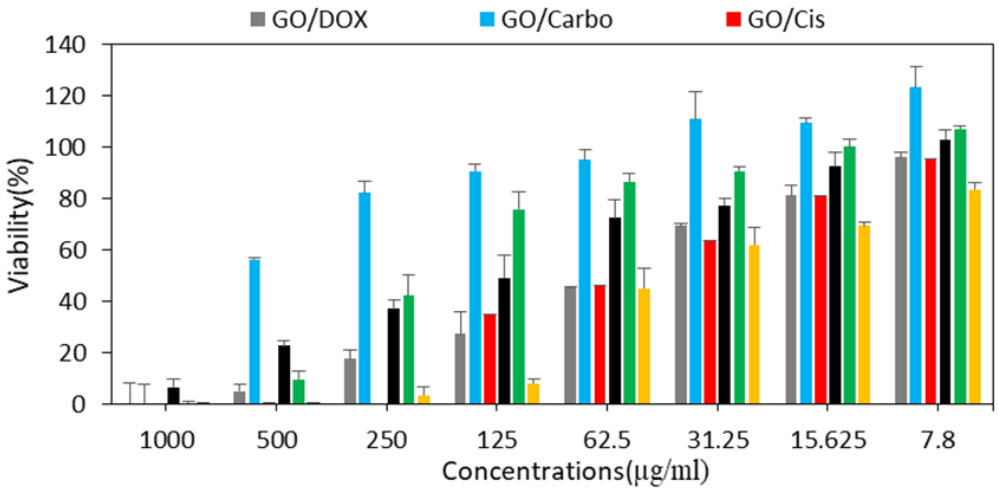

Fig. 6 – Antibacterial properties of of GO/DOX, GO/carbo, GO/Cis, rGO/DOX, rGO/Carbo and RGO/Cis at different concentrations against *Escherichia coli*.

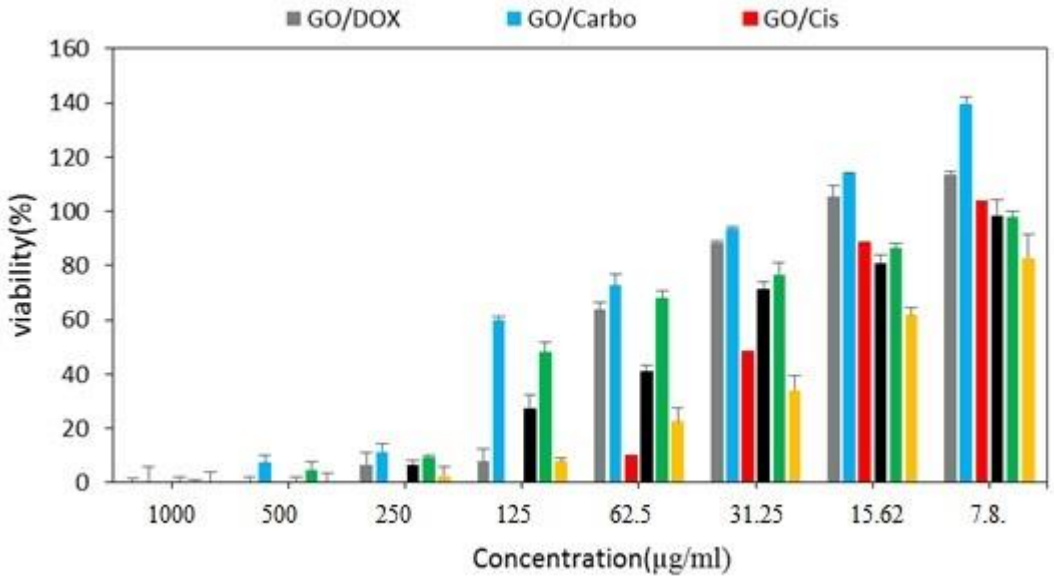

Fig. 7 – The effect of Cis-containing samples on the survival of MCF-7 line cells.

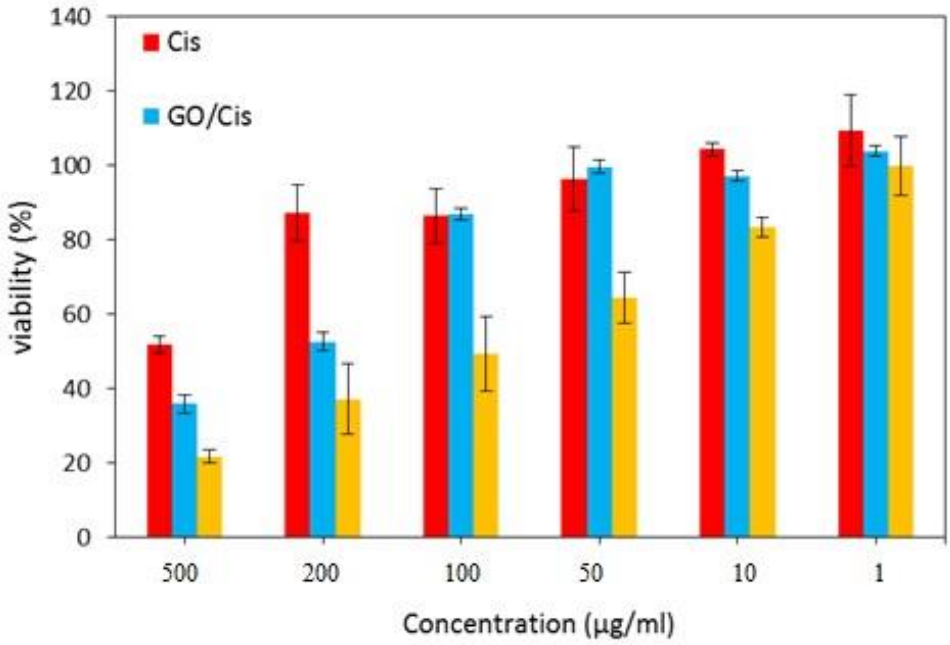

Fig. 8 – Effect of DOX-containing formulations at different concentrations on the survival of MCF-7 line cells.

The survival rate of MCF-7 cells relative to the three compounds DOX, GO/DOX and rGO/ DOX is shown in Fig. 6. Here, too, as shown, the cell viability decreased with increasing sample concentration.

In this series of samples, rGO/DOX sample showed higher toxicity than DOX and GO/DOX samples. This was especially noticeable for concentrations above 100 µg/mL. The lowest cell viability with a value of 21.76 is related to the rGO/DOX sample at a concentration of 500 µg/mL and the highest cell viability with a value of 117.44 is related to the DOX sample at a concentration of 1µg/mL.

Fig. 7 shows the effect of Carbo-containing samples on MCF-7 cell viability in the concentration range of 1 to 500 µg/mL. The two samples GO/Carbo and rGO/Carbo were less toxic than DOX and had a higher cell viability in equal concentrations. The best results were related to rGO/Carbo sample and the lowest cell viability was observed in DOX with a concentration of 500 µg/mL.

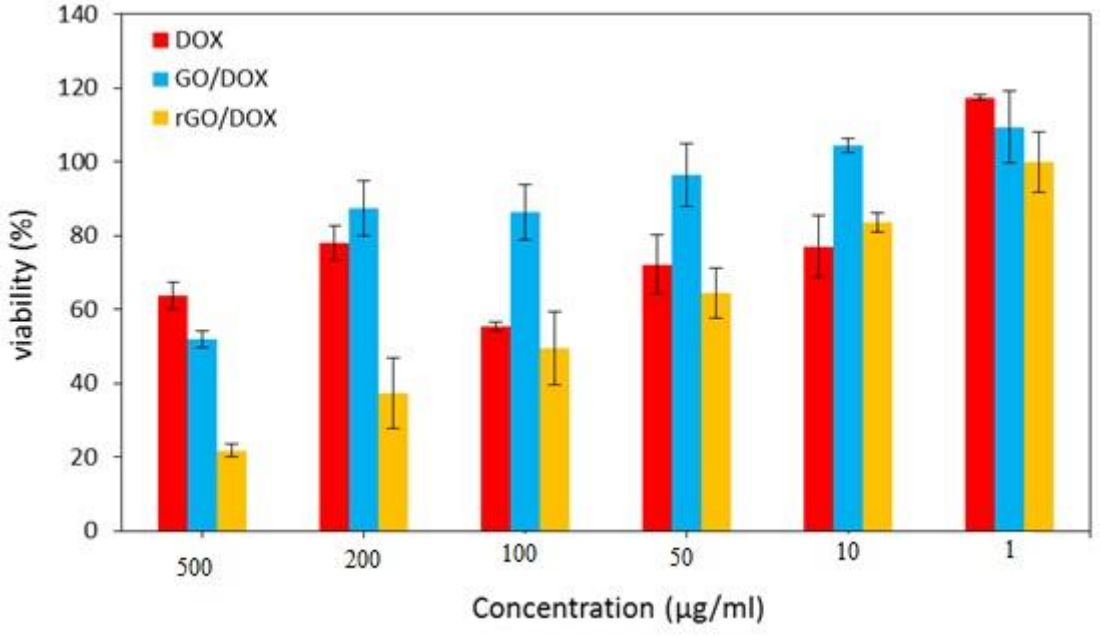

Fig. 9 – Effect of Carbo-containing formulations at different concentrations on MCF-7 cell viability.

CONCLUSIONS

The bacteria *Corynebacterium* and *Enterococcus* behave similarly to *Staphylococcus*. The difference was that the rate of increase in life of these bacteria in response to low concentrations was significantly increased. These two bacteria also showed the greatest reduction in viability against RGO/Cis up to 125 and 62.5 µg/mL, respectively, and also with a similar argument can confirm the antibacterial behavior of this compound.

Acknowledgements. The authors are thankful to the Ahvaz Branch, Islamic Azad University and the Shiraz Branch, Islamic Azad University for partial support of this work.

REFERENCES

1. N. Sree Harsha, R. Maheshwari, B.-E. Al-Dhubiab, M. Tekade, M. C. Sharma and K. N. Venugopala, *Int. J. Nanomed.*, **2019**, *14*, 7419.
2. N. Ma, J. Liu, W. He, Z. Li, Y. Luan and Y. Song, *J. Colloid Interface Sci*., **2017**, *490*, 598.
3. Y. Ye, X. Mao, J. Xu, J. Kong and X. Hu, *Int. J. Polym. Sci*., **2019**, *2019*, Article ID 8453493.
4. S. Priyadarsini, S. Mohanty, S. Mukherjee, S. Basu and M. Mishra, *J. Nano. Str. Chem.*, **2018**, *8*,123.
5. L. Lerra, A. Farfalla, B. Sanz, G. Cirillo, O. Vittorio and M. Le Grand, *Pharmaceutics*, **2019**, *11*, 3.
6. D. Huang and D. Wu, *Mater. Sci. Eng.* C, **2018**, *90*, 713.
7. V. Agarwal and P. B. Zetterlund, *Chem. Eng. J*., **2021**, *405*, 127018.
8. K. Thakur and B. Kandasubramanian, *J. Chem. Eng. Data*, **2019**, *64*, 833.
9. H. Ahmad, M. Fan and D. Hui, *Engineering*, **2018**, *145*, 270.
10. Z. Ismail, *Ceram. Int*., **2019**, *45*, 23857.
11. G. Behbudi, *Adv. in Appl. Nano. Bio-Tech*., **2020**, *1*, 63.
12. F. Farjadian, S. Abbaspour, M. A. A. Sadatlu, S. Mirkiani, A. Ghasemi and M. Hoseini Ghahfarokhi, *Chem. Sel*., **2020**, *5*, 1020010219.
13. X. Zhao, Z. Wei, Z. Zhao, Y. Miao, Y. Qiu and Y. Yang, *ACS Appl. Mater. Interfaces*, **2018**, *10*, 6608.
14. W. Ma, H. Yang, Y. Hu and L. Chen, *Polym Int.*, **2021**, *70*, 1413.
15. U. Kanwal, N. I. Bukhari, N. F. Rana, M. Rehman, K. Hussain and N. Abbas, *Int. J. Nanomedicine*., **2018**, *14*. 1.
16. A. Jabbar, G. Yasin, W. Q. Khan, M. Y. Anwar, R. M. Korai and M. N. Nizam, *RSC Adv*., **2017**, *7*, 31100
17. S. Song, H. Shen, Y. Wang, X. Chu, J. Xie and N. Zhou, *Colloid Sand Surf B: Biointerfaces*, **2020**, *185*, 110596.
18. W. Yu, L. Sisi, Y. Haiyan and L. Jie, *RSC Adv*., **2020**, *10*, 15328.
19. E. L. Westman, M. J. Canova, I. J. Radhi, K. Koteva, I. Kireeva, N. Waglechner and G. D. Wright, *Chem Biol*., **2012**, *26*, 1255.